

PAPER • OPEN ACCESS

Numerical simulation of a novel expanded metal tubular structure for crashworthiness application

To cite this article: A H A Abdelaal and F Tarlochan 2015 *IOP Conf. Ser.: Mater. Sci. Eng.* **100** 012063

View the [article online](#) for updates and enhancements.

You may also like

- [Investigation on crashworthiness and mechanism of a bionic antler-like gradient thin-walled structure](#)
Zhiquan Wei, Xu Zhang and Yang Zheng
- [Optimized foam filling configuration in bi-tubular crush boxes: a comprehensive experimental and numerical analysis](#)
Hamidreza Salaripoor, Mohammadbagher B Azimi and Masoud Asgari
- [Crashworthiness of automobile made of HDPE/kenaf and HDPE/MWCNT polymer composites](#)
Nayan Pundhir, Himanshu Pathak and Sunny Zafar

ECS Toyota Young Investigator Fellowship



For young professionals and scholars pursuing research in batteries, fuel cells and hydrogen, and future sustainable technologies.

At least one \$50,000 fellowship is available annually.
More than \$1.4 million awarded since 2015!



Application deadline: January 31, 2023

Learn more. Apply today!

Numerical simulation of a novel expanded metal tubular structure for crashworthiness application

A H A Abdelaal¹ and F Tarlochan¹

¹Mechanical and Industrial Engineering Department, College of Engineering, Qatar University, PO Box 2713 Doha, Qatar

E-mail: faris.tarlochan@qu.edu.qa

Abstract. Search for new geometries and materials that would serve in crashworthiness applications is a cumulative process. Recent studies investigated the performance of expanded metal tubes and the possible ways to enhance its energy absorption capability. The aim of this work is to investigate the crashworthiness characteristics of new concept is proposed where expanded metal tube is suited into a double-walled tube made of the same material to form one structure. The tube was then numerically tested through a verified model using ABAQUS software. Moreover, the influence of the size of the expanded metal cell was also investigated in the present study. The new concept showed an enhanced energy absorption characteristics related to the change in the mass of the tubular structure. The enhancement was related to both the change in deformation pattern, and the increase in crushed mass.

1. Introduction

Number of factors makes thin-walled structures one of the most widely used structures for crashworthiness applications. These structures are relatively cheap, light and capable of absorbing high amount of energy through a stable progressive collapse. During collision thin-walled structures are plastically deformed and fractured what leads to the dissipation of collision's kinetic energy [1]. The term "Crashworthiness" was adopted by the automotive safety community to describe the occupant's safety performance afforded by all types of motor vehicles in different accident types. Meeting automotive industry standards made researchers and engineers look for methods to enhance the energy absorption capacity without increasing structure weight in their design of the energy absorbers. For this reason, maximizing specific energy absorption (SEA, amount of energy absorbed per unit mass) and attaining a unity value for crush force efficiency (CFE, the ratio of the average crushing force to the maximum force) are namely the main objectives in the design of thin-walled structures for crashworthiness applications [2]. A set of factors influence these performance indicators that can be summarized in first: the material properties represented in Young's modulus, yield stress, and strain hardening. Second factor is the geometry of the energy absorber. The geometry parameters could be the walls' thickness, cross-section width or diameter. Other factor is the initial imperfections like having patterns, corners, grooves or indentations in the structure [3].

Numerous studies have been published on the crushing response of empty and foam-filled tubular structures. The effect of internal geometries on the energy absorption performance of simple extruded profiles was explained thoroughly in studies [4-13]. Introducing multi-cellular structures to the column generally enhance the energy absorption performance of tubular structures [8]. Multi-cellular structures are mostly simple extruded profiles that can fill the tube partially or fully.



In studies [12-21] the influence of outer geometry of simple thin-walled structures on energy absorption characteristics was studied. Such geometries are mainly classified into prismatic and non-prismatic members. The studies have shown that the energy absorption of thin-walled structures depends greatly on the cross-section of structure. In addition, increasing the perimeter to a certain limit shows higher energy absorption capability in most of the tested profiles [1].

Studying the energy absorption characteristics of thin-walled structures under impact was conducted both numerically and experimentally. Studies [22-24] showed that findings of numerical and experimental studies had almost matching results with inconsiderable variation.

The aforementioned solutions are limited to the available manufacturing techniques commonly used in producing thin-walled structures. Even the most recent studies in the area of crashworthiness applications are still focused on simple geometries. With the advancement in manufacturing techniques like Direct Metal Laser Sintering (DMLS) it is now possible to produce complex geometries that can be integrated to the thin-walled structures. DMLS functions by melting metal powder layer by layer in a high vacuum with electron beam. This technology produces dense parts from metal powder with characteristics of target material what makes it a powerful tool in producing complex 3D shapes and parts.

A continuous effort is made in investigating new materials and geometries that could improve the performance of tubular structures in crashworthiness applications. Very few information about the performance of expanded metal tubes is found in the literature. The process of manufacturing expanded metal sheets is achieved through an in-line expansion of partially slit metal sheets. The outcome of this process is a diamond-like pattern shown in Figure 1. Paper [25] summarizes the international patents on expanded metal. Major advantage of expanded metal sheets is its ability to absorb energy under different loading conditions like bending, shear, or axial compression. The use of concentric tubes in [3] showed a significant enhancement to both energy absorption capability and mean load due to the interaction between both tubes during collision. The aim of the present work is to investigate other possible mechanisms to further enhance the energy absorption of expanded metal tubes.

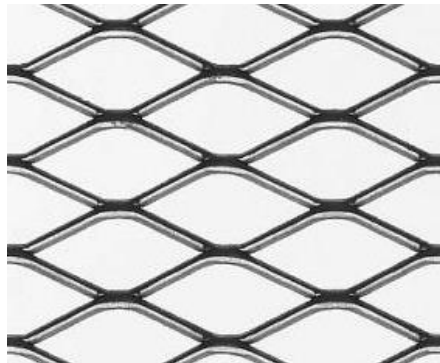


Figure 1. Typical expanded metal sheet.

1.1. Crashworthiness Indicators

To indicate the crashworthiness performance the overall crash response was considered. Different variables were obtained to characterize the overall crash response:

1.1.1. Peak Load. Peak load is the maximum force observed in the effective stroke of the tubular structure during impact. It is important to determine this value as it indicates possible consequences or damages that could be seen by the body being protected.

1.1.2. Energy Absorption. The total energy absorption E in a crash test equals the area under the load-displacement curve. It is defined as equation (1).

$$E = \int_0^{d_{max}} F ds \quad (1)$$

For simplicity, d_{max} or stroke efficiency is taken to be $0.75L$ where L is the tube length. To relate how much energy a structure can absorb to its mass, specific energy absorption is obtained. It is defined as equation (2).

$$SEA = \frac{E}{m} \quad (2)$$

Where m is the crushed mass of the component.

1.1.3. Crushing Force Efficiency. The crushing force efficiency is a ratio between the mean and peak crushing force, the two parameters that are related to the deceleration occurring during a crash. It is defined as equation (3).

$$CFE = \frac{P_{mean}}{P_{max}} \quad (3)$$

An ideal energy absorber would have a CFE value close to one. That is because an ideal absorber would preserve a peak load for its entire crushed length.

2. Design Methodology

Findings of [3] showed that the deformation of expanded metal tubes lead to unstable structural response. In an attempt to solve this issue, expanded metal tube was fit in-between two metal sheets as shown in figure 2. A schematic view of an expanded metal cell is shown in figure 3. The major dimensions are the two orthogonal axis, l_1 and l_2 , width (w), and thickness (t) of the expanded metal cell. The values are tabulated in table 1 for the different proposed designs. The thin-walled tube has a cross-sectional area of 80×80 mm and an overall thickness of 2.0 mm. The tube's length is chosen as 350 mm to assure the full potential deformation of the tube when it is crashed. Material assigned to all designs is A36 mild-steel. The test is conducted through an axial impact on the tubular structure using a striker of 275 kg mass with an initial velocity of 15.6 m/s as shown in figure 4.

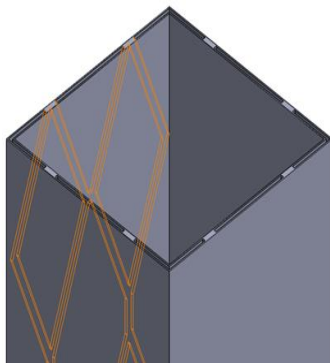


Figure 2. Design concept.

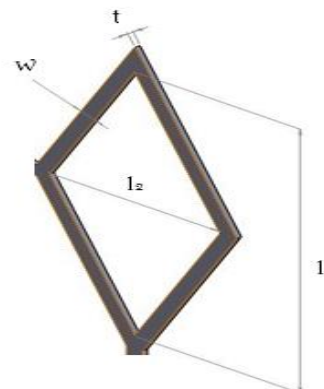

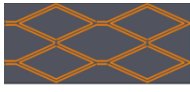
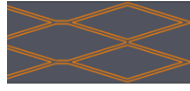

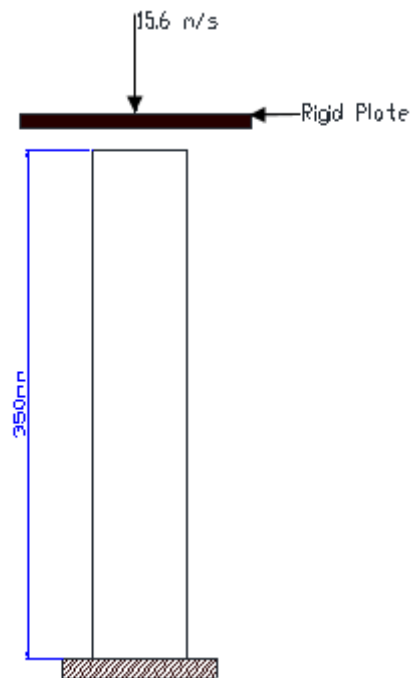


Figure 3. Schematic view of an expanded metal cell.

Table 1. Geometry and dimensions of structures under study.

Specimen ID	Expanded Metal Sheets Dimensions				Tube Dimensions			Profile
	l_1 (mm)	l_2 (mm)	w (mm)	t (mm)	Length (mm)	Perimeter (mm)	Mass (g)	
S1	35.68	31.22	2.74	1	350	320	1000	
S2	72.60	32.50	2.74	1	350	320	919	
S3	108.97	32.78	2.74	1	350	320	976	
S4	146.91	32.88	2.74	1	350	320	973	

**Figure 4.** Simulation test setup.

2.1. Finite Element Model

To find the continuum point's time dependent deformation equation (4) is used.

$$\sigma_{ij} + \rho f_i = \rho \ddot{x}_i \quad (4)$$

Where, σ_{ij} represents the Cauchy stress, ρ is the density, f_i is the body force and \ddot{x}_i is the acceleration. Using the divergent theorem equation (4) can be transformed into the virtual work principle given in equation (5).

$$\int_V \rho x_i \delta \ddot{x}_i dV + \int_V \sigma_{ij} \delta x_{ij} dV - \int_V \rho f_i \delta x_i dV - \int_{S^2} t_i \delta x_i dS = 0 \quad (5)$$

Equation (5) can be written in matrix form as shown in equation (6).

$$\sum_{i=1}^n \left\{ \int_V \rho N^t N a dv + \int_V B^t \sigma dv - \int_V \rho N^t b dv - \int_A N^t F dA + \int_s N^t F_c ds \right\}^i = 0 \quad (6)$$

Where the number of elements is expressed as n , the stress column vector as σ , the interpolation matrix as N , the nodal acceleration vector as a , the body load column vector as b and the applied traction force as F . A general way to explain the matrix form is stated in equation (7).

$$[M] \left[\frac{d^2 u}{dt^2} \right] + [C] \left[\frac{du}{dt} \right] + [K] \{U\} = [F(t)] \quad (7)$$

Where M , C and K are the mass, damping and stiffness matrices respectively.

First the initial and boundary condition are considered. Then the displacements are solved according to these conditions. After the displacements solution is obtained, the computation of other variables such as plastic strains, force and energies starts. The mentioned equation is usually solved by finite element software using implicit methods. However, explicit methods are desired for nonlinear dynamic problems like the crash test in our case. The main idea of such explicit methods is the division of total time into small time intervals or steps. Desired dynamic equations are solved and their variables are evaluated at increment $t+1$ based on knowing their previous values at t . The major difference between the explicit and implicit methods is that current step dependency. In implicit methods the evaluation of a step one relies on the information of the previous step and the current one where in explicit methods it only depends on the previous step value. This dependency on the current step value makes solving such equations harder, thus explicit methods are used in such cases.

In this work the finite element model for thin-walled tube with the employed complex geometries were generated using ABAQUS. The non-linear finite element code ABAQUS explicit was used to predict the response of the tube and its complex structures after it is impacted by a plate of certain mass with certain velocity. To model the first section of the tubular structure, a square tube of 80.0 x 80.0 mm, 350.0 mm length and 2.0 mm thickness is first modeled with a groove that goes through the total length on the tube with a thickness of 1.0 mm, inside this groove an expanded metal tube is modeled. A better picturing of the tube would be double walled tube with expanded metal cells in-between. The thin walled tube was modelled using 4 node shell continuum (S4R) element with reduced integration points. The shell elements size is selected to be 2.50 mm. The top plate (striker) was modeled as a rigid body with a reference point mass of 275 kg and with a predefined velocity field of 15.6 m/s on one of its reference point. The motion of the top plate was restricted to only translational motion along the tube's axes. The thin walled tube is fixed on the lower rigid plate using a constraint between their two surfaces. To account for the contact between the two plates and the tube, a general contact algorithm is chosen with a penalty coulomb friction coefficient of 0.2 [26]. This is to avoid the interpenetration between the tube walls.

To account for the structure materials, the A-36 mild-steel models were adopted and verified from [1]. The steel verified mode showed 2% deviation from the one in [1], and thus it was used in the simulation for this study. The mild-steel has a young modulus $E=200$ GPa and Poisson's ratio of 0.3.

The plastic behavior of the steel was modeled using Johnson-Cook model with the parameters shown in table 2.

Table 2. Johnson-Cook parameters [1].

Parameters	Values
A	146.7 MPa
B	896.9 MPa
Strain Power Coefficient, N	0.32
C	0.033
Temperature Power Coefficient, M	0.323
Reference Strain Rate	1.0 s ⁻¹
Density	7850 kg/m ³
Melting temperature, T _m	1773 K
Specific Heat, C _p	486 J/kg-K

3. Results and Discussion

3.1. Force-displacement characteristics and deformation patterns.

Figures 5 and 6 show the force-displacement curves for the four numerically tested samples of the present study. The displacement represents the change in position of the striker which was brought to a full contact with tube at the test beginning. Samples with the same force-displacement curve features were grouped together to simplify the analysis.

The deformation pattern of S2 is very similar to S4 with a slight phase-out of the location at which folds starts to form. Force of S2 is generally larger than S4 as more interaction is happening between the expanded metal sheets and the double-walled tube.

The behavior of S1 and S3 is different as the number of expanded metal cells is higher in the case of S1 sample leading to formation of more folds. Observing the deformed tubes shows that S1 had the most stable collapse among tested samples. This is also evident in the value of CFE. Compared to models where expanded metal sheets is solely used in forming the tubular structure, the outward buckling has not occurred for any of the tested tubes as the double-walled tube controls the deformation of the expanded metal sheets. In all tested sample, progressive collapse starts with the formation of regular lobes then some irregularity starts to appear at the end of the effective stroke length.

Table 3. Summary of crashworthiness parameters for studied concepts.

	E (kJ)	SEA (kJ/kg)	P _{Mean} (kN)	P _{Max} (kN)	CFE (%)
S1	12.1	16.1	46.4	121.1	38.3
S2	5.2	7.6	20.1	118.4	17.0
S3	10.7	14.6	41.2	129.8	31.7
S4	9.9	13.6	38.0	130.4	29.1

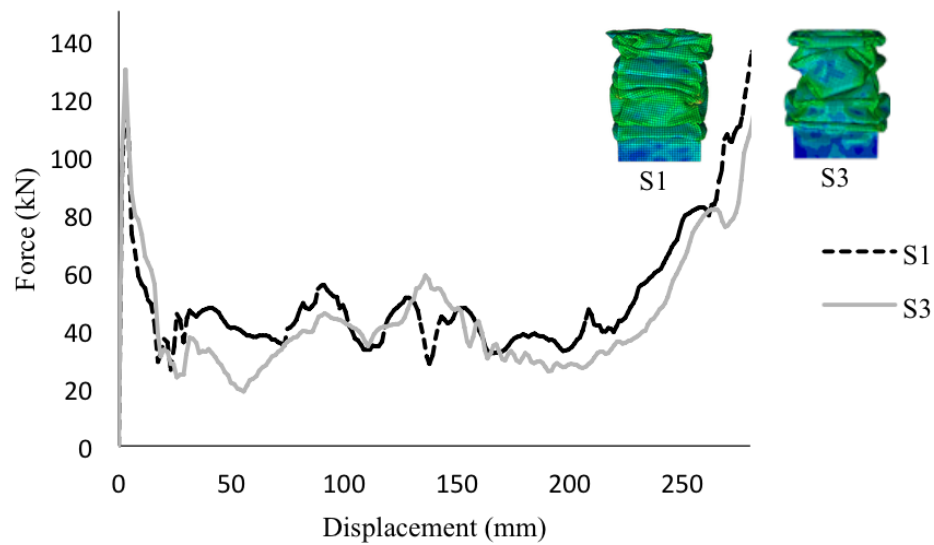


Figure 5. Crushing force vs. displacement curves for S1 and S3 models.

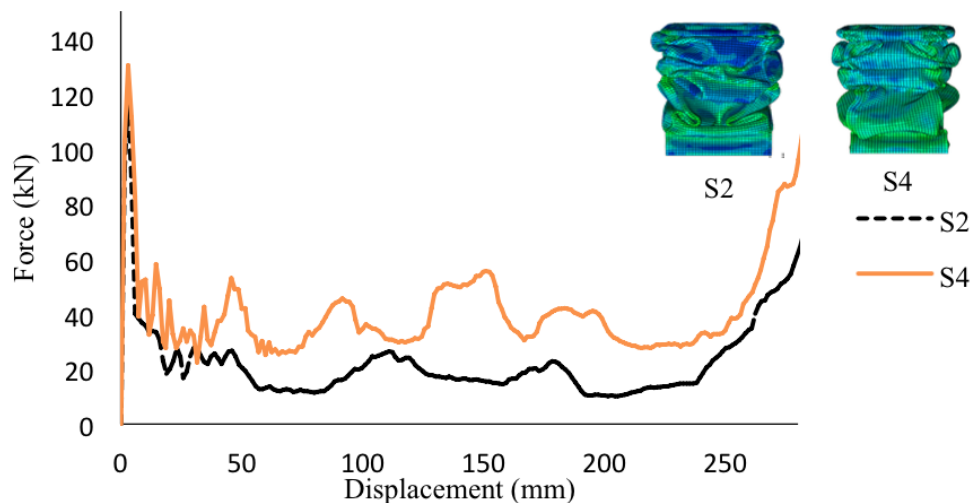


Figure 6. Crushing force vs. displacement curves for S2 and S4 models.

3.2. Energy Absorption

In figure 7, the energy absorption is plotted as a function of the deformation length of the different structural design concepts. From these figures, it can be seen that S1 with the smallest cell size attained the highest energy absorption value among tested samples.

The relation between cell size and energy absorption isn't clear in figure 7. However, a closer look at other factors affecting the energy absorption shows that as the total mass of the tube increases the energy absorption increases as well. This is demonstrated in figure 8. In this particular case, increasing the mass of the tube increases the deformed mass and enhances the energy absorption performance of the tube with a minimum influence of cell size on the energy absorption characteristics. Finally, comparing the present models with the ones presents in [21] and of the same mass and overall thickness shows a significant enhances in energy absorption capabilities of the tubular structure.

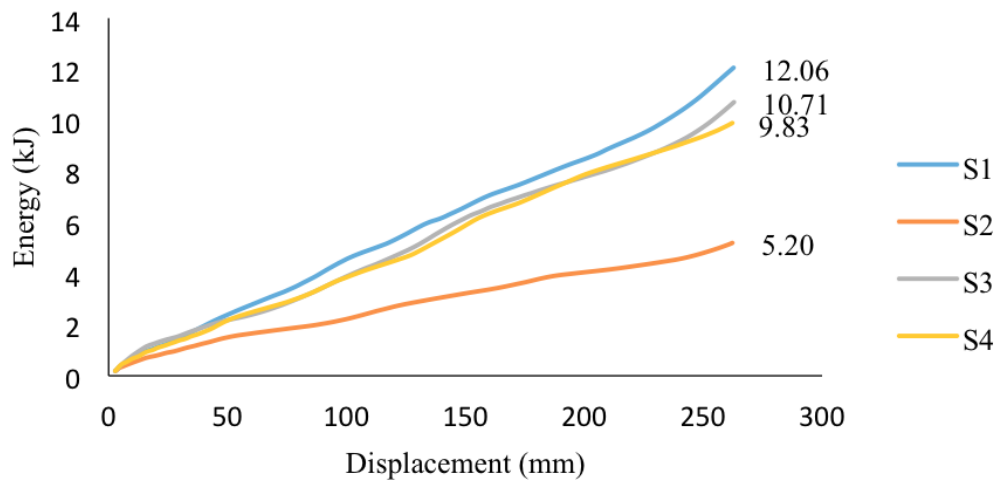


Figure 7. Energy vs. displacement for studied concepts.

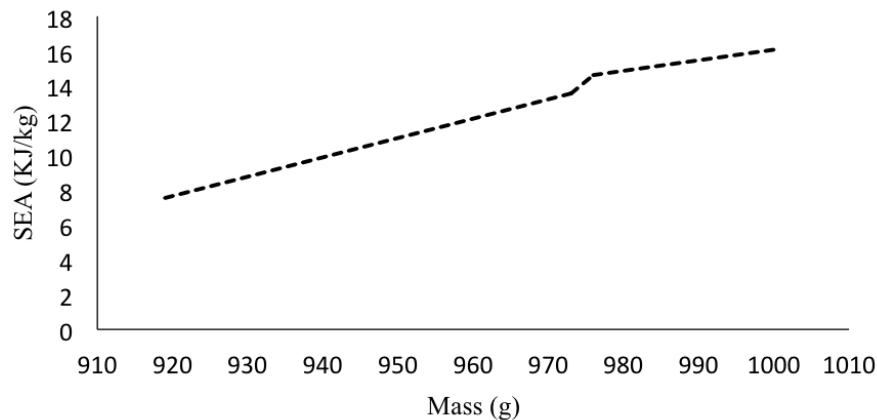


Figure 8. SEA vs. tube mass of studied concepts.

4. Conclusion

In this study, expanded metal sheet was placed between the two sides of a double-walled tube made of the same material. Crushing of the tubes was conducted numerically through a verified model on ABAQUS software. It was observed that the proposed design enhanced the energy absorption over ordinary expanded metal tubes. The major reason for that is the change in the deformation modes that leads to a progress folding during the collision instead of outwards buckling. Such behavior results from the restriction caused by the double-walled tube. Increasing the cell size by varying the two orthogonal axis showed no correlation to the energy absorption; however, the tubes with more mass regardless of the size of their cells showed better energy absorption compared to the ones with less mass. Further work needs to be done to understand the influence of expanded metal cells thickness on the performance of the tubes for the same cell size and double-walled tube overall wall thickness.

Acknowledgement

The authors would like to appreciate the efforts of Qatar University in providing all necessary support.

References

- [1] Tarlochan F, Samer F, Hamouda A, Ramesh S, Khalid K 2013 *Thin-Walled Structures* **71** 7-17
- [2] Tang Z, Liu S, Zhang Z 2013 *Thin-Walled Structures* **62** 75-84
- [3] Smith D, Graciano C, Martínez G 2014 *Thin-Walled Structures* **84** 170-6

- [4] Ajdari A, Nayeb-Hashemi H, Vaziri A 2011 *International Journal of Solids and Structures* **48** 506-16
- [5] Hanssen A, Langseth M, Hopperstad O 2001 *International Journal of Mechanical Sciences* **43** 153-76
- [6] Hanssen A G, Langseth M, Hopperstad O S 2000 *International Journal of Impact Engineering* **24** 347-83
- [7] Sun G, Li G, Hou S, Zhou S, Li W, Li Q 2010 *Materials Science and Engineering: A* **527** 1911-9
- [8] Zhang X, Cheng G 2007 *International Journal of Impact Engineering* **34** 1739-52
- [9] Mahdi E, Sebaey T 2014 *Thin-Walled Structures* **76** 8-13
- [10] Tasdemirci A, Kara A, Turan K, Sahin S 2015 *Thin-Walled Structures* **91** 116-28
- [11] Sharifi S, Shakeri M, Fakhari H E, Bodaghi M 2015 *Thin-Walled Structures* **89** 42-53
- [12] Nia A A, Parsapour M 2014 *Thin-Walled Structures* **74** 155-65
- [13] Liu S, Tong Z, Tang Z, Liu Y, Zhang Z 2015 *Thin-Walled Structures* **88** 70-81
- [14] Shahi V J, Marzbanrad J 2012 *Thin-Walled Structures* **60** 24-37
- [15] Nagel G, Thambiratnam D 2004 *International journal of mechanical sciences* **46** 201-16
- [16] Reddy S, Abbasi M, Fard M 2015 *Thin-Walled Structures* **94** 56-66
- [17] Abbasi M, Reddy S, Ghafari-Nazari A, Fard M 2015 *Thin-Walled Structures* **89** 31-41
- [18] Malekzadeh P, Daraie M 2014 *Thin-Walled Structures* **84** 1-13
- [19] Zhang X, Wen Z, Zhang H 2014 *Thin-Walled Structures* **84** 263-74
- [20] Tanlak N, Sonmez F O 2014 *Thin-Walled Structures* **84** 302-12
- [21] Smith D, Graciano C, Martínez G, Teixeira P 2014 *Thin-Walled Structures* **85** 42-9
- [22] Yin H, Wen G, Liu Z, Qing Q 2014 *Thin-Walled Structures* **75** 8-17
- [23] Abedrabbo N, Mayer R, Thompson A, Salisbury C, Worswick M, Van Riemsdijk I 2009 *International Journal of Impact Engineering* **36** 1044-57
- [24] Ahmad Z, Thambiratnam D, Tan A 2010 *International Journal of Impact Engineering* **37** 475-88
- [25] Smith D, Graciano C, Martínez G 2009 *Recent Patents on Materials Science* **2** 209-25
- [26] Dehghan-Manshadi B, Mahmudi H, Abedian A, Mahmudi R 2007 *Materials & design* **28** 8-15